

Preparation of Fe-substituted Mesoporous Silicas with Highly Isolated Iron Species in Buffer Solution

XIN Hong-Chuan, TANG Jian-Ting, FAN Feng-Tao, YANG Qi-Hua, LI Can

(State Key Laboratory of Catalysis, Dalian Institute of Chemical Physics, Chinese Academy of Sciences, Dalian 116023, China)

Abstract: The iron-substituted mesoporous silicas were synthesized under mild acidic conditions ($\text{pH} = 4.4$, HOAc-NaOAc buffer solution) using tetramethoxysilane (TMOS), tetraethoxysilane (TEOS) or sodium silicate solution as silica source in the presence of block copolymer pluronic P123 as the mesoporous template. TMOS and sodium silicate led to iron-containing silicas with ordered two-dimensional hexagonal mesoporous structure, and vesicle mesostructure was obtained using TEOS as silica precursor. UV-Vis and UV resonance Raman spectra show that highly isolated iron species can be predominantly obtained on mesoporous iron-containing silicas synthesized using inexpensive sodium silicate and $\text{Fe}(\text{NO}_3)_3$ as precursors. The buffer solution provides a facile strategy for controlling the mesostructure of iron-containing silicas by simply varying the silica source. Mesoporous iron-substituted silicas are highly efficient in hydroxylation of phenol because of a high dispersion of active iron centers within silica matrices and a high accessibility of active iron species to reactants.

Key words: Fe-SBA-15; isolated iron species; sodium silicate; hydrothermal; UV resonance Raman spectroscopy

Iron-substituted microporous zeolites have attracted much attention due to their remarkable activity as catalysts for the selective oxidation of hydrocarbons. However, one obvious shortcoming of these zeolite catalysts (such as Fe/ZSM-5) is that their active sites in micropores are not very accessible to bulky reactants in fine chemical and pharmaceutical industries. Compared with zeolite, mesoporous silicas with large pore diameter, high surface area and ordered pore arrangement, can be used as the supports in chemical reactions involving bulky molecules.

Iron-containing mesoporous silicas are of increasing interest due to their potential applications as efficient heterogeneous catalysts in many catalytic reactions^[1-2]. The iron species (*i.e.* oxidation states and coordination environment) have great effects on their catalytic performance^[3]. It is very important to prepare mesoporous silicas incorporated with specific uniform iron species in order to obtain high catalytic performance.

Normally strong acidic and basic synthesis conditions cannot afford mesoporous iron-containing silicas such as Fe-MCM-41 and Fe-SBA-15 with uniform and high content of iron species, due to the easy formation of iron oxide in basic medium and easy dissolution of iron

ions in acidic medium, respectively^[4-7]. Under neutral conditions, it was reported that high content of iron species could be incorporated in the framework of Fe-HMS^[8]. However, it is still difficult to synthesize highly ordered mesostructure at pH value above 3. Therefore, it is a challenge to develop a facile route for the preparation of SBA-15-type mesoporous iron-containing silicas with high content of highly isolated iron species.

Recently we have reported the synthesis of transition-metal (Fe, Ti, *etc.*) containing mesoporous silicas with high content of highly isolated metal species in buffer solution using TEOS and sodium silicate as precursors^[9-10]. However, the matching of hydrolysis and condensation rates between the two silica sources and one metal source makes the system complex. It is very interesting to simplify this synthesis route and have fundamental scientific understanding of the definite interaction behaviors between silica source and iron source in mild buffer medium, during the synthesis of mesoporous iron-containing silicas. Herein, we systematically investigated the influence of different silica sources (TMOS, TEOS, sodium silicate) on the properties of Fe-substituted mesoporous silicas and developed an opti-

Received date: 2009-06-29, **Modified date:** 2009-08-19, **Published online:** 2009-08-28

Foundation item: The Programme Strategic Scientific Alliances between China and the Netherlands (2008DFB50130); National Basic Research Program of China (2009CB623503, 2005CB221407)

Biography: XIN Hong-Chuan (1977 -), male, PhD candidate. E-mail: hexin@dicp.ac.cn

Corresponding author: YANG Qi-Hua, professor. E-mail: yangqh@dicp.ac.cn; LI Can (1960 -), professor. E-mail: canli@dicp.ac.cn

mized hydrothermal synthesis route to obtain highly isolated iron species, using cost-effective inorganic starting materials, under environmental-friendly hydrothermal conditions.

1 Experimental

All materials were of analytical grade and used as received without any further purification. Triblock poly (ethylene oxide)-poly (propylene oxide)-poly (ethylene oxide) copolymer Pluronic P123 ($\text{EO}_{20}\text{PO}_{70}\text{EO}_{20}$) was purchased from Sigma-Aldrich Company Ltd. (USA). Tetramethoxysilane (TMOS), tetraethoxysilane (TEOS), $\text{Fe}(\text{NO}_3)_3 \cdot 9\text{H}_2\text{O}$, sodium silicate solution (20wt% SiO_2 , 6wt% Na_2O), and other reagents were obtained from Shanghai Chemical Reagent. Inc. of Chinese Medicine Group.

In a typical synthesis, 1.00g P123 and 1.69g ethanol were dissolved in 28mL HOAc-NaOAc buffer solution ($\text{pH}=4.4$, 0.52mol/L HOAc, 0.27mol/L NaOAc) at 25°C under vigorous stirring. Then a solution with 17mmol silica source (TMOS or TEOS) and 0.25mmol $\text{Fe}(\text{NO}_3)_3 \cdot 9\text{H}_2\text{O}$ in 1.69g ethanol was added. In the case of sodium silicate as silica source, 17mmol sodium silicate solution was added to the above surfactant solution, followed by stirring at 25°C for 10min and then addition of a solution with a certain amount of $\text{Fe}(\text{NO}_3)_3 \cdot 9\text{H}_2\text{O}$ in 1.69g ethanol. The resultant mixture was stirred at 40°C for 20h and aged at 100°C under static conditions for additional 24h. The powder product was recovered by filtration and dried at 100°C for 4h. The surfactant was removed by calcination of as-synthesized material at 550°C for 10h in air. The calcined material was denoted as Fe-Si- n ($n=25, 50, 75, 100$), where Si refers to silica source, and n refers to 0.25, 0.50, 0.75 or 1.00mmol iron source added. For example, Fe-NaSiO-50 refers the material synthesized with sodium silicate as silica source, 0.50mmol $\text{Fe}(\text{NO}_3)_3 \cdot 9\text{H}_2\text{O}$ as iron source. In order to investigate the effect of buffer solution, a material was synthesized in the same procedure as Fe-NaSiO-50, using 28mL HCl solution ($\text{pH}=4.4$) instead of 28mL HOAc-NaOAc buffer solution ($\text{pH}=4.4$). This material was denoted as Fe-NaSiO-50-HCl.

X-ray diffraction (XRD) patterns were recorded on a Rigaku RINT D/Max-2500 powder diffraction system using $\text{CuK}\alpha$ radiation of 0.15406nm wavelength. The nitrogen sorption experiments were performed at -196°C on a Micromeritics ASAP 2020 system. Prior to the

measurement, the materials were out gassed at 120°C for at least 6h. The Brunauer-Emmett-Teller (BET) specific surface areas were calculated using the adsorption data in the relative from pressure (P/P_0) range of 0.05 ~ 0.25. Pore size distributions were calculated using the Barrett-Joyner-Halenda (BJH) method based on the adsorption branch. The total pore volumes were estimated from the amounts adsorbed at a relative pressure P/P_0 of 0.99. Transmission electron microscopy (TEM) was performed using a JEOL JEM-2000EX at an acceleration voltage of 120kV. UV-Vis diffuse reflectance spectra were recorded on a JASCO V-550 UV-Vis spectrophotometer. The powder material was loaded into a quartz cell, and the spectra were collected in the range from 190nm to 800nm with BaSO_4 as the reference. UV resonance Raman spectra were collected at room temperature with a Jobin-Yvon T64000 triple-stage spectrograph with a spectral resolution of 2cm^{-1} . The 257nm line from a Coherent Innova 300 Fred laser was used as an excitation source in the deep UV region. The power of the 257nm line at the material was below 1.0mW. The elemental analysis was determined by ICP-AES after the material was dissolved in a mixture of HF and HNO_3 .

The phenol hydroxylation was carried out as reported previously^[9]. In a standard reaction, 0.470g phenol and 0.047g catalyst were added to 15mL deionized water in a two-neck flask fitted with a condenser. Hydrogen peroxide (H_2O_2 , 30wt% aqueous solution) was added through a syringe to the magnetically stirred phenol solution containing catalyst at 60°C ($n(\text{phenol}):n(\text{H}_2\text{O}_2)=3:1$). The reaction were analyzed on HPLC Agilent 1100 (Agilent Technologies, Waldbronn, Germany) equipped with C8 column (4.6mm \times 150mm). The products were separated on the column using a methanol/water mixture ($V(\text{methanol}):V(\text{water})=40:60$) as the mobile phase at the flow rate of 1.0mL/min with UV detection at 277nm. The identification and quantification of reactant and products were performed using standard compounds (phenol, hydroquinone and catechol).

2 Results and Discussion

2.1 Effect of silica source on the structure and iron species of mesoporous iron-containing silicas

Figure 1(a) shows the XRD patterns of Fe-Si-25 materials. The XRD pattern of Fe-TMOS-25 shows three diffraction peaks in the low angle range from 0.8° to 2° , which can be indexed to the (100), (110), and (200)

reflections of a hexagonal symmetry lattice. Fe-TEOS-25 synthesized with TEOS as silica source gives a single peak at low diffraction angle together with a broad shoulder. Fe-NaSiO-25 shows two low-angle diffractions in the XRD pattern. Figure 2 shows the TEM images of Fe-Si-25 materials. The TEM image of Fe-TMOS-25 has ordered 2-D hexagonal mesostructure (Fig. 2(a)) as we reported previously^[11], consistent with the XRD result. Vesicle could clearly be observed in the TEM image of Fe-TEOS-25 (Fig. 2(b)). For the material synthesized with sodium silicate as silica source, Figure 2(c) and Fig. 2(d) show the TEM images of Fe-NaSiO-25 taken along the parallel channels and vertical to the parallel channels, respectively. The TEM images confirm ordered parallel cylindrical pore channels, in accordance with the XRD result.

Figure 1(b) shows the nitrogen sorption isotherms of Fe-Si-25. The corresponding textural properties are summarized in Table 1. For all materials, type IV isotherms with steep H1 hysteresis loops at relative pressure P/P_0 of 0.5 ~ 0.8 can be observed, implying the formation of uniform large mesopores. For Fe-TMOS-25 and Fe-TEOS-25, they have similar BET surface area (about 800m²/g), and the BET surface area of Fe-NaSiO-25 is 444m²/g.

The iron contents of Fe-Si-25 (Table 1) are similar (0.88wt% ~ 0.96wt%) and slightly lower than the theoretical content (1.32wt%), indicating almost stoichiometric incorporation of iron species in mild acidic buffer solution.

The coordination environment of iron species was characterized using UV-Vis diffuse reflectance spectroscopy (Fig. 3(a)). The UV-Vis spectrum of Fe-Si-25 mainly shows a strong absorption peak centered at 245nm and a shoulder peak at 220nm, which can be assigned to ligand-to-metal charge transfer band of isolated tetrahe-

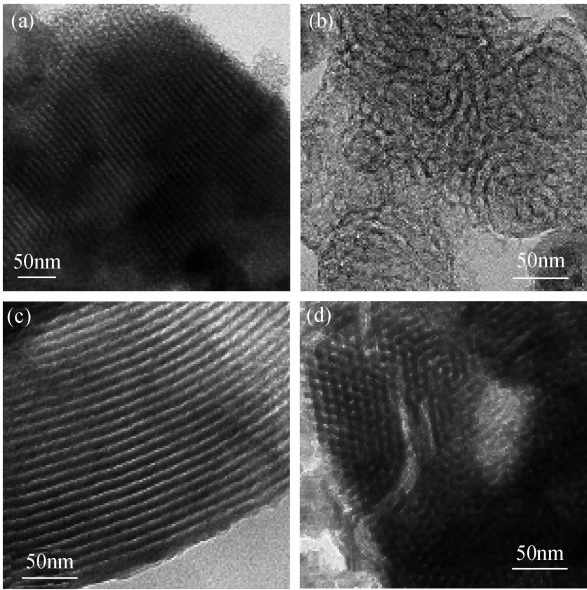


Fig. 2 TEM images of Fe-TMOS-25 (a), Fe-TEOS-25 (b) and Fe-NaSiO-25 (c, d)

drally coordinated Fe³⁺ in [FeO₄]^{-[12]}. No significant absorption peak is observed above 320nm for Fe-NaSiO-25, suggesting that the material is free of iron oxide oligomer or ferric oxide species^[13]. But for Fe-TMOS-25 and Fe-TEOS-25, obvious absorption above 320nm can be observed, indicating that under current mild acidic synthesis system, using TMOS or TEOS as silica source may readily form more undesirable aggregated iron species. The color of Fe-NaSiO-25 is white, but the color of Fe-TMOS-25 and Fe-TEOS-25 is yellow, indicating that mainly uniform and isolated iron species exist in Fe-NaSiO-25, which is in accordance with the results of UV-Vis spectra.

These results show that sodium silicate favors the formation of isolated iron species compared with TEOS and TMOS. The influence of silica source on the coordination environment of iron species in the mesoporous framework could be attributed to the difference in hydrolysis rate and condensation rate of different silica sources.

UV resonance Raman spectroscopy is a very powerful technique to characterize transition-metal ions in the framework of zeolites and mesoporous silicas^[14-15]. With UV line excitation, low fluorescence interference and strong resonance Raman enhancement make it possible for the sensitive detection of isolated Fe species in mesoporous iron-containing silicas. A 257nm laser line was used as the excitation line, which is close in energy to the CT band of Fe—O as indicated in the UV-Vis spectra (Fig. 3(a)), and hence, resonance Raman spectra should be obtained for the Fe species in the materials.

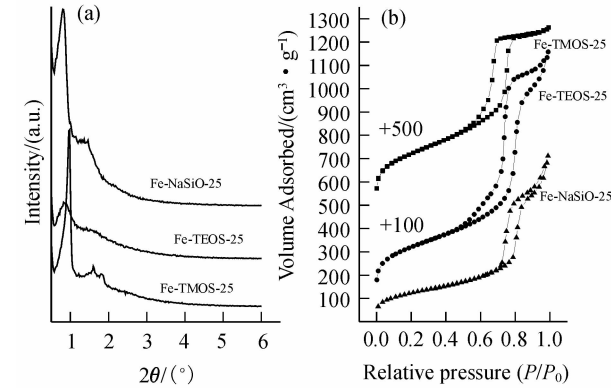


Fig. 1 XRD patterns (a) and nitrogen sorption isotherms (b) of Fe-Si-25

Table 1 Structural parameters of material Fe-Si-*n*

Material	Fe /wt%	S_{BET} /($\text{m}^2 \cdot \text{g}^{-1}$)	V_t /($\text{cm}^3 \cdot \text{g}^{-1}$)	D_{BJH} /nm
Fe-TMOS-25	0.92	803	1.18	8.2
Fe-TEOS-25	0.96	793	1.64	10.2
Fe-NaSiO-25	0.88	444	1.10	10.7
Fe-NaSiO-50	1.51	357	1.08	11.4
Fe-NaSiO-75	2.22	481	1.16	10.7
Fe-NaSiO-100	2.65	532	1.13	9.9
Fe-NaSiO-50-HCl	n. d.	29	0.09	—

Figure 3 (b) shows the UV-Raman spectrum of Fe-NaSiO-25. The bands at 510 and 1090 cm^{-1} are the resonance Raman bands associated with the isolated iron species in the framework of the materials, assigned to the Fe-O-Si symmetric and asymmetric stretching mode of the isolated tetrahedral iron ions in the silica framework, respectively^[6,9]. The band at 978 cm^{-1} is associated with the Si-O-Si bond near the framework iron species or other defect sites such as the surface silanol group^[16].

The combinatorial results of XRD, UV-Vis spectra, nitrogen sorption, UV Raman spectra and elemental analyses show that ordered mesoporous iron-containing silicas with uniform isolated iron species can be synthesized directly under mild acidic conditions. The large pore size (9 – 12 nm) of these materials may facilitate the mass transport of bulky substrates and also bulk products.

Most of the work deals with synthesis of mesoporous silica materials using TMOS or TEOS as silica source. These alkoxides are convenient as starting materials but they are expensive and the products can only find applications where price is not a major issue. Therefore, preparation of mesoporous silicas from cost-effective inorganic sources, such as water glass is attractive in view of

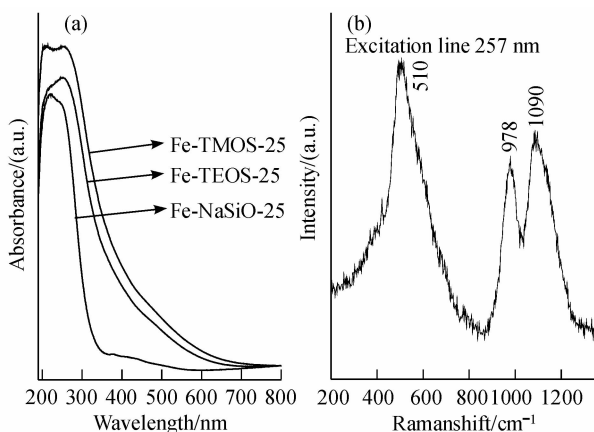


Fig. 3 UV-Vis spectra of Fe-Si-25 (a) and UV-Raman spectrum of Fe-NaSiO-25 (b)

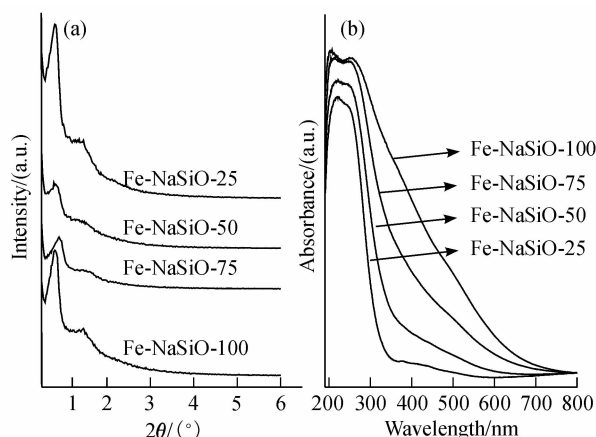


Fig. 4 XRD patterns (a) and UV-Vis spectra (b) of Fe-NaSiO-*n* industrial scale-up fabrication of mesoporous silica materials.

2.2 Effect of iron loading on the structure and iron species of mesoporous iron-containing silicas

In order to investigate the effect of iron loading on the structure and iron species, we prepared Fe-NaSiO-*n* with different iron contents. Figure 4 (a) shows the XRD patterns of Fe-NaSiO-*n*. All materials exhibit two diffractions in their low-angle XRD patterns, indicating that they are all ordered mesoporous materials, and have similar meso-structures.

The corresponding textural properties are also summarized in Table 1. The nitrogen sorption results indicate that, Fe-NaSiO-*n* materials have similar BET surface area (357 – 532 m^2/g) and pore volume (1.08 – 1.16 cm^3/g), indicating that the iron content does not alter the textural structure greatly.

The iron content of Fe-NaSiO-*n* increases with the amount of $\text{Fe}(\text{NO}_3)_3$ in the initial mixture (Table 1). Figure 4 (b) shows the UV-Vis spectra of Fe-NaSiO-*n*. The increasing of iron content leads to the gradual increase of absorption at higher wavelength, indicating that more and more aggregated iron species are generated. Uniform highly isolated iron species can only be obtained when iron loading is below 1.51 wt%, which is much higher than previous mesoporous iron-containing silicas synthesized under strong acidic conditions^[5]. This implies that the capacity to accommodate uniform highly isolated iron species is not unlimited in current hydrothermal system, where mild acidic buffer solution serves as the medium.

2.3 Effect of buffer solution on the structure and iron species of mesoporous iron-containing silicas

In order to investigate the effect of buffer solution on the structure and iron species of the final materials, we

employed aqueous HCl solution with same pH value for comparison.

The XRD pattern of Fe-NaSiO-50-HCl (not shown) shows no diffraction peak in the low-angle region, indicating that no ordered mesostructure was obtained. The textural properties of Fe-NaSiO-50-HCl from nitrogen sorption are summarized in Table 1. The BET surface area and total pore volume are 29m²/g and 0.09cm³/g, respectively, much lower than the mesoporous counterpart, Fe-NaSiO-50. The acidity of aqueous HCl medium is easily altered after addition of basic sodium silicate solution, due to its lack of buffering capability. Therefore, the whole system becomes very basic, which makes the condensation of sodium silicate around P123 micelles ineffectively. This indicates that the mild buffer solution plays an important role in the formation of the mesoporosity in the current synthesis system.

Figure 5 shows the UV-Vis spectra of these two materials. The spectra indicate that uniform highly isolated iron species can also be obtained when aqueous HCl solution with same acidity is employed.

Aqueous HCl medium is normally used in the synthesis of mesoporous materials when triblock copolymer as the template under acidic conditions^[17]. The employment of HOAc-NaOAc buffer, instead of HCl solution, avoids the water contamination from Cl⁻ during filtration of as-synthesized materials after hydrothermal treatment. The final pH value of the product solution is nearly neutral, also prevents the production of corrosive wastewater. In this aspect, this is an environmentally benign synthesis procedure, especially for the potential scale-up industrial application

The current procedure presents a cost-effective and environmentally friendly strategy for the preparation of ordered Fe-containing mesoporous silicas, and more interestingly, may provide opportunities for the synthesis of

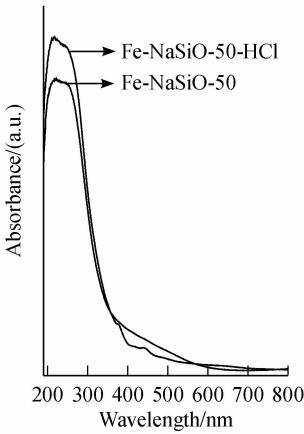


Fig. 5 UV-Vis spectra of Fe-NaSiO-50 and Fe-NaSiO-50-HCl

Table 2 Hydroxylation of phenol catalyzed by Fe-NaSiO-50 and Fe-NaSiO-50-HCl using H₂O₂ as oxidant

Material	C ₆ H ₆	Diphenol	H ₂ O ₂	H ₂ O ₂
	Conv. /%	Sel. /%	Conv. /%	Sel. /%
Fe-NaSiO-50	26.1	60.9	69.4	68.3
Fe-NaSiO-50-HCl	4.6	0	0	0

other transition metal-substituted mesoporous analogues where in high content of uniform active species are expected to be incorporated.

2.4 Effect of mesoporosity on the performance of phenol hydroxylation

Hydroquinone (HQ) and catechol (CAT) are widely used in chemical, pharmaceutical and food industries^[9].

In order to investigate the effect of mesoporosity of the materials on the catalytic performance, we carried out the phenol hydroxylation over Fe-NaSiO-50 and Fe-NaSiO-50-HCl with similar iron content and iron species as discussed above. The reaction results are shown in Table 2. The by-product is mainly the over oxidative products of the phenol such as black tarry. Fe-NaSiO-50-HCl cannot efficiently catalyze the phenol hydroxylation to form desirable products (CAT and HQ). However, for Fe-NaSiO-50, very good catalytic performance was obtained with 26.1% conversion of phenol and 60.9% selectivity of CAT and HQ, which is comparable to the iron-containing catalysts reported previously^[9,18]. This big difference in catalysis indicates that the mesoporosity (total pore volume is 1.08cm³/g for Fe-NaSiO-50) of the material makes the active sites dispersed on a high surface area (BET surface area is 357m²/g for Fe-NaSiO-50) and more accessible to reactants (*i. e.* phenol and hydrogen peroxide). It is obvious that the mesoporous materials can benefit a high dispersion of catalytically active centers over a large surface area, and therefore, a high accessibility to reactants in catalytic reactions.

3 Conclusions

In summary, an optimized synthesis procedure has been developed to prepare mesoporous iron-containing silicas with highly dispersed iron species under mild acidic conditions. Sodium silicate as silica source makes the synthesis of mesoporous silica materials cost-effective. Buffer solution (pH = 4.4, HOAc-NaOAc) as the synthesis medium makes the synthesis process envi-

ronmentally friendly and the formation of mesoporosity feasible using sodium silicate under such mild acidic conditions. The mesoporosity of iron-containing silicas has great advantages of a good dispersion of active sites and a desirable accessibility to reactants in the catalytic reaction of phenol hydroxylation.

References:

- [1] Wang Y. *Res. Chem. Intermediat.*, 2006, **32**(3/4): 235-251.
- [2] Li Y, Feng Z C, van Santen R A, *et al.* *J. Catal.*, 2008, **255**(2): 190-196.
- [3] Xin H C, Yang Q H. *Petrochem. Tech.*, 2006, **35**(11): 1017-1024.
- [4] Yuan Z Y, Liu S Q, Chen T H, *et al.* *J. Chem. Soc. Chem. Commun.*, 1995(9): 973-974.
- [5] Li Y, Feng Z C, Lian Y X, *et al.* *Micropor. Mesopor. Mater.*, 2005, **84**(1/2/3): 41-49.
- [6] Li Y, Feng Z C, Xin H C, *et al.* *J. Phys. Chem. B*, 2006, **110**(51): 26114-26121.
- [7] Han Y, Meng X J, Guan H B, *et al.* *Micropor. Mesopor. Mater.*, 2003, **57**(2): 191-198.
- [8] Tuel A, Arcon I, Millet J M M. *J. Chem. Soc. Faraday Trans.*, 1998, **94**(23): 3501-3510.
- [9] Xin H C, Liu J, Fan F T, *et al.* *Micropor. Mesopor. Mater.*, 2008, **113**(1/2/3): 231-239.
- [10] Tang J T, Liu J, Yang J, *et al.* *J. Colloid Interf. Sci.*, 2009, **335**(2): 203-209.
- [11] Liu J, Yang Q H, Zhang L, *et al.* *Adv. Funct. Mater.*, 2007, **17**(4): 569-576.
- [12] Mohapatra S K, Sahoo B, Keune W, *et al.* *Chem. Commun.*, 2002(14): 1466-1467.
- [13] Li Y, Xia H A, Fan F T, *et al.* *Chem. Commun.*, 2008(6): 774-776.
- [14] Li C. *J. Catal.*, 2003, **216**(1/2): 203-212.
- [15] Li C. *Stud. Surf. Sci. Catal.*, 2007, **170**: 561-576.
- [16] Xiong G, Li C, Li H Y, *et al.* *Chem. Commun.*, 2000(8): 677-678.
- [17] Zhao D Y, Huo Q S, Feng J L, *et al.* *J. Am. Chem. Soc.*, 1998, **120**(24): 6024-6036.
- [18] Choi J S, Yoon S S, Jang S H, *et al.* *Catal. Today*, 2006, **111**(3/4): 280-287.

缓冲溶液中制备掺杂高度隔离铁物种的介孔氧化硅

辛洪川, 汤建庭, 范峰滔, 杨启华, 李 灿

(中国科学院 大连化学物理研究所 催化基础国家重点实验室, 大连 116023)

摘要: 使用 P123 作为模板剂, 采用不同的硅源(正硅酸甲酯, 正硅酸乙酯, 硅酸钠)在弱酸性的条件下 ($\text{pH} = 4.4$, 乙酸-乙酸钠缓冲溶液) 合成掺杂铁的介孔氧化硅材料. 正硅酸甲酯和硅酸钠形成有序的二维六方相的介孔结构, 而正硅酸乙酯形成了囊泡结构. 紫外可见漫反射光谱和紫外共振拉曼光谱表明, 在环境友好的条件下, 采用硝酸铁和硅酸钠可以合成出高度隔离的铁物种. 缓冲溶液提供了一条便捷的途径, 通过简单改变硅源来控制介孔结构. 掺杂铁的介孔氧化硅材料在苯酚的羟化反应中表现出优异的催化性能, 主要由于铁物种高度分散在氧化硅载体上, 介孔结构使铁活性位更易于接近反应物分子.

关键词: Fe-SBA-15; 隔离铁物种; 硅酸钠; 水热合成; 紫外共振拉曼光谱

中图分类号: TQ174

文献标识码: A